

Refractometric sensor based on whispering-gallery modes of thin capillaries

Vanessa Zamora, Antonio Díez, Miguel V. Andrés and Benito Gimeno

Departamento de Física Aplicada - ICMUV, Universidad de Valencia, Dr. Moliner 50, 46100 Burjassot, Spain
miguel.andres@uv.es

Abstract: Whispering-gallery modes resonances of submicron wall thickness capillaries exhibit very large wavelength shifts as a function of the refractive index of the medium that fills the inside. The sensitivity to refractive index changes is larger than in other optical microcavities as microspheres, microdisks and microrings. The outer surface where total internal reflection takes place remains always in air, enabling the measure of refractive index values higher than the refractive index of the capillary material. The fabrication of capillaries with submicron wall thickness has required the development of a specific technique. A refractometer with a response higher than 390 nm per refractive index unit is demonstrated. These sensors are readily compatible with microfluidic systems.

©2007 Optical Society of America

OCIS codes: (230.4000) Microstructure fabrication; (230.5750) Resonators; (170.4520) Optical confinement and manipulation; (240.6690) Surface waves; (290.3030) Index measurements; (060.2370) Fiber optics sensors.

References and links

1. A. B. Matsko and V. S. Ilchenko, "Optical resonators with whispering-gallery modes—Part I: Basics," *IEEE J. Sel. Top. Quantum Electron.* **12**, 3-14 (2006).
2. V. S. Ilchenko and A. B. Matsko, "Optical resonators with whispering-gallery modes—Part II: Applications," *IEEE J. Sel. Top. Quantum Electron.* **12**, 15-32 (2006).
3. A. Kiraz, A. Kurt, M. A. Dündar and A. L. Demirel, "Simple largely tunable optical microcavity," *Appl. Phys. Lett.* **89**, 081118 (2006).
4. M. Borselli, T. J. Johnson and O. Painter, "Beyond the Rayleigh scattering limit in high-Q silicon microdisks: theory and experiment," *Opt. Express* **13**, 1515-1530 (2005).
5. M. Hossein-Zadeh and K. J. Vahala, "Free ultra-high-Q microtoroid: a tool for designing photonic devices," *Opt. Express* **15**, 166-175 (2007).
6. S. Arnold, M. Khoshshima, I. Teraoka, S. Holler and F. Vollmer, "Shift of whispering-gallery modes in microspheres by protein adsorption," *Opt. Lett.* **28**, 272-274 (2003).
7. C. Y. Chao and L. J. Guo, "Biochemical sensors based on polymer microrings with sharp asymmetrical resonance," *Appl. Phys. Lett.* **83**, 1527-1529 (2003).
8. S. Y. Cho and N. M. Jokerst, "A polymer microdisk photonic sensor integrated onto silicon," *IEEE Photon. Technol. Lett.* **18**, 2096-2098 (2006).
9. A. Díez, M. V. Andrés and J. L. Cruz, "Hybrid surface plasma modes in circular metal-coated tapered fibers," *J. Opt. Soc. Am. A* **16**, 2978-2982 (1999).
10. N. M. Hanumegowda, C. J. Stica, B. C. Patel, I. White and X. Fan, "Refractometric sensors based on microsphere resonators," *Appl. Phys. Lett.* **87**, 201107 (2005).
11. A. Yalçın, K. C. Papat, J. C. Aldridge, T. A. Desai, J. Hryniewicz, N. Chbouki, B. E. Little, O. King, V. Van, S. Vhu, D. Gill, M. Anthes-Washburn, M. S. Ünlü and B. B. Goldberg, "Optical sensing of biomolecules using microring resonators," *IEEE J. Sel. Top. Quantum Electron.* **12**, 148-155 (2006).
12. *Handbook of Chemistry and Physics*, R. C. Weast, M. J. Astle and W. H. Beyer, ed. (CRC Press, Boca Raton 1986-1987), pp. E374-E375.
13. I. M. White, H. Oveys and X. Fan, "Liquid-core optical ring-resonator sensors," *Opt. Lett.* **31**, 1319-1321 (2006).
14. I. M. White, H. Oveys, X. Fan, T. L. Smith and J. Zhang, "Integrated multiplexed biosensors based on liquid core optical ring resonators and antiresonant reflecting optical waveguides," *Appl. Phys. Lett.* **89**, 191106 (2006).
15. I. M. White, H. Zhu, J. D. Suter, N. M. Hanumegowda, H. Oveys, M. Zourob and X. Fan, "Refractometric sensors for Lab-on-a-chip based on optical ring resonators," *IEEE Sens. J.* **7**, 28-35 (2007).

16. C. A. Balanis, *Advanced Engineering Electromagnetics* (John Wiley & Sons, 1989), Chap. 6.
 17. I. D. Chremmos, N. K. Uzunoglu and G. Kakarantzas, "Rigorous analysis of the coupling between two nonparallel optical fibers," *J. Lightwave Technol.* **24**, 3779-3788 (2006).
 18. R. P. Kenny, T. A. Birks and K. P. Oarkley, "Control of optical fibre taper shape," *Electron. Lett.* **27**, 1654-1656 (1991).
 19. J. C. Knight, G. Cheung, F. Jacques and T. A. Birks, "Phase-matched excitation of whispering-gallery mode resonances by a fiber taper," *Opt. Lett.* **22**, 1129-1131 (1997).
 20. T. A. Birks, J. C. Knight and T. E. Dimmick, "High-resolution measurement of the fiber diameter variations using whispering gallery modes and no optical alignment," *IEEE Photon. Technol. Lett.* **12**, 182-183 (2000).
 21. J. Carmon, L. Yang and K. J. Vahala, "Dynamical thermal behavior and thermal self-stability of microcavities," *Opt. Express* **12**, 4742-4750 (2004).
-

1. Introduction

Dielectric optical microcavities based on whispering-gallery modes (WGM) are remarkable devices with a wide range of applications as filters, lasers, sensors and modulators [1,2]. These monolithic resonators may exhibit ultra-high Q values, very small volume, high mechanical stability and good compatibility with integrated optics. Continuous advances in micro- and nano- fabrication technologies [3-5] drive a fast growth of their applications for the three basic geometries, i.e., spheres, disks and rings.

Highly sensitive refractometer, based on WGM resonances, for chemical and biological applications have been demonstrated. In these applications, WGM resonances of microspheres [6], microrings [7] and microdisks [8] shift as a function of the external refractive index that surrounds the microcavities. A typical experimental arrangement involves the immersion of the microcavities in a liquid medium and this imposes an upper limit to the maximum value of the refractive index of the liquid. The refractive index of the microcavity dielectric determines that limit, as in other evanescent field sensors [9], since the total internal reflection cancels out when the refractive index of the liquid exceeds such a limit.

The response of these resonators in terms of wavelength shift per refractive index unit (RIU) is typically below 100 nm/RIU (30 nm/RIU was reported in [10] using microsphere resonators and 140 nm/RIU was reported in [11] using microring resonators). When the response is calibrated using a glucose solution (concentration measured by the weight percent), then the typical response is 0.1 nm/% [7,8], which corresponds to 70 nm/RIU [12].

The alternative that we propose is to exploit WGM resonances of thin capillaries where the analyte fills the inside of the capillaries. These resonators exhibit a unique property, i.e., the spatial separation between the surface where the total internal reflection takes place and the sensing surface, where the wave interacts with the medium that contains the analyte. Thus, when a liquid fills a capillary, the resonances shift as a function of the refractive index of the liquid, while the external medium remains air. As we will show, this permits to sense liquids with a refractive index higher than that of the capillary material, which is an outstanding property. Previous published results based on capillaries [13-15] show a relatively low response (between 10 and 20 nm/RIU), which is due to the use of capillaries with a relatively thick wall (between 3 and 6 μm). Here, we present a technique to prepare thin silica capillaries with submicron wall thickness and we demonstrate that the response can be 100 times higher. Thus, the WGM resonances of thin silica capillaries exhibit a response higher than microspheres and microrings, permit the use of liquids with high refractive index and are readily compatible with microfluidic systems.

2. Theoretical simulations

The simulations that we present here have been carried out solving Maxwell equations with boundary conditions for a dielectric system with cylindrical symmetry [16], as in previous analysis [13,15]. The WGM resonances that we study are waves that propagate in the azimuthal direction with an axial propagation factor equal to zero. The spectrum of these resonances splits into the two well known TM^z and TE^z series, which correspond to the modes

that have the axial component of the magnetic field or the electric field equal to zero, respectively. Eventually, a more rigorous 3D simulation could be carried out following the analysis of the coupling between two nonparallel fibers [17].

The external radius of the capillary, a , determines the wavelength separation between two consecutive resonances of azimuthal order m ($\Delta\lambda \approx \lambda^2/(n2\pi a)$, where n is the silica refractive index). If we want a reasonable separation, to avoid overlapping and to reduce any possible mistake when measuring refractive index changes, then a small radius a is needed. For example, a radius of 5 μm will give a separation between resonances of about 50 nm. However, as the free spectral range (FSR) is increased, the Q factor reduces.

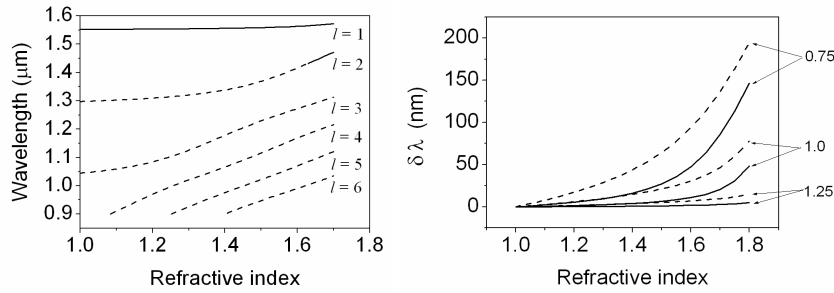


Fig. 1. (Left) TM^z WGM resonances wavelength of azimuthal order $m = 25$ and radial order l , $a = 5 \mu\text{m}$ and $d = 1 \mu\text{m}$, versus the internal refractive index (the dashed lines denote a Q factor lower than 500). (Right) Wavelength shift for both TM^z (solid line) and TE^z (dashed line) resonances of azimuthal order $m = 25$, radial order $l = 1$ and $a = 5 \mu\text{m}$, for three values of the wall thickness ($d = 1.25, 1.00$ and $0.75 \mu\text{m}$), versus the internal refractive index.

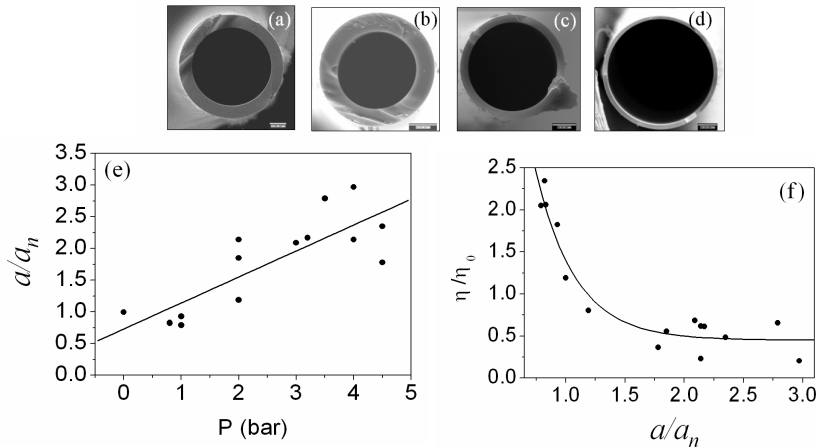


Fig. 2. SEM image of four capillaries: (a) $a = 76 \mu\text{m}$, $d = 20 \mu\text{m}$ (example of a capillary before tapering), (b) $a = 9.9 \mu\text{m}$, $d = 3.1 \mu\text{m}$ (example of a capillary tapered down without pressurization), (c) $a = 5.5 \mu\text{m}$, $d = 0.8 \mu\text{m}$ (example of a submicron wall thickness capillary tapered with a pressure of 2 bar) and (d) $a = 7.5 \mu\text{m}$, $d = 0.45 \mu\text{m}$ (another example of submicron wall thickness capillary tapered with a pressure of 2 bar). (e) Relative radius a/a_n versus the pressure applied to the capillary. (f) Normalized ratio $\eta = d/a$ versus the relative radius a/a_n .

Figure 1(left) gives the wavelength of the TM^z WGM resonances with azimuthal order $m = 25$, as a function of the internal refractive index, for a silica capillary with an external radius $a = 5 \mu\text{m}$ and a wall thickness $d = 1 \mu\text{m}$. This plot includes the lower radial order resonances, $l = 1, 2, \dots$, and shows that for small external radius and wall thickness only the first resonance exhibits a relatively high Q factor and consequently only this resonance will be observed in the experiments. A similar spectrum is obtained for the TE^z WGM resonances.

Figure 1(right) gives the computed response, i.e., wavelength shift as a function of the internal refractive index, for the fundamental ($l = 1$) TM^z and TE^z resonances of azimuthal order $m = 25$ and for a capillary with radius $a = 5 \mu\text{m}$ and three values of wall thickness d . These simulations demonstrate that the use of submicron thickness capillaries is crucial to achieve a high sensitivity. The slope computed for the TE^z resonance, when $d = 0.75 \mu\text{m}$, is 150 nm/RIU at 1.3 refractive index value, i.e., around the value corresponding to water solutions, and 360 nm/RIU at 1.6.

Although we have focused our analysis on the advantages of using submicron thickness capillaries, we should point out that by increasing the external radius a further improvement on both the slope and the Q-factor should be obtained [15]. However, a simultaneous decrease of the free spectral range would be caused.

3. Fabrication of thin capillaries

The capillaries are prepared in two steps. First, we reduce the dimensions of commercial Suprasil 300 silica tubes of about 10 mm diameter to obtain capillaries with a diameter around 100 μm . This first step is carried out using the furnace of an optical fiber pulling tower. Then, in a second step, we reduce further the radius of the capillaries using a fusion and pulling technique. The elongation speed and flame temperature that we use are the same that are used when tapering standard optical fiber [18]. However, for preparing submicron wall thickness capillaries it is necessary to pressurize the capillaries by pumping an inert gas in them while they are tapered. Thus, our technique insures optimum optical quality of the outer surface of the capillaries, since it avoids the use of chemical etching to reduce the dimensions.

Figure 2 gives the results of an experimental study in which a number of capillaries have been tapered down at constant flame temperature and elongation speed. The initial radius of these capillaries was within the range 40 - 80 μm . The capillaries were tapered to obtain a uniform diameter waist of 6 mm long with a nominal radius a_n between 2 and 10 μm . Here we refer as nominal radius to the radius that would be obtained if a solid rod were tapered. Thus, the deviations of the final radius a with respect to the nominal radius are due to the combined effects of surface tension of the hole and the pressure applied during the fusion and pulling process. In Fig. 2(e) we can see that the relative radius a/a_n increases linearly with pressure, and easily reaches values above 2, demonstrating capillary inflation with a relatively low pressure. Likewise, in Fig. 2(f) we plot the ratio $\eta = d/a$, normalized with its initial value before tapering, $\eta_0 = (d/a)_0 = 0.26$. Now we see that a reduction factor of 0.5 can be reached when the capillary inflation exceeds a relative radius $a/a_n = 2$. Figure 2 includes SEM pictures of some capillaries to summarize the results of this study and to give two examples of submicron wall thickness capillaries. In fact, in section 4 we give a complete characterization of the capillary depicted in Fig. 2(c).

4. Experimental characterization

The excitation of the WGM resonances was achieved using an optical fiber tapered down to 1 μm diameter [19]. Figure 3 gives a scheme of the experimental arrangement. The transmission spectra were recorded using a broadband light source and an optical spectrum analyzer with 1 nm resolution. A fiber polarizer and a polarization controller were used to adjust the input polarization in order to excite separately each eigenstate of polarization. Figure 3 includes, as an example, two spectra recorded for TE^z and TM^z polarization, corresponding to a capillary, with $a = 5.5 \mu\text{m}$ and $d = 0.8 \mu\text{m}$, filled with a liquid. Each WGM resonance exhibits a tail of weaker resonances at slighter shorter wavelengths that can be identified as spiral modes [20].

Using a set of calibrated Cargille fluids, we have carried out a full characterization of several capillaries as refractometric sensors. Figure 4 gives the wavelength shift of both TE^z and TM^z WGM resonances as a function of the nominal refractive index values of the Cargille fluids, for two capillaries: one with $a = 5.5 \mu\text{m}$ and $d = 0.8 \mu\text{m}$ and the other with a smaller external radius $a = 4.5 \mu\text{m}$ and a similar wall thickness $d = 0.8 \mu\text{m}$.

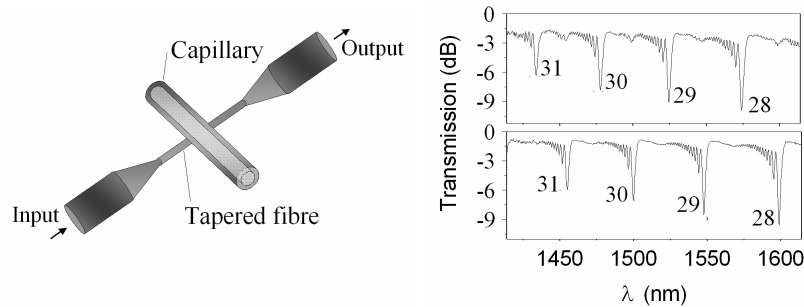


Fig. 3. (Left) Scheme of the experimental arrangement. (Right) Transmission spectra for the TE^z (top) and TM^z (bottom) WGM resonances and for a refractive index of 1.52. Each resonance is identified with its azimuthal order m .

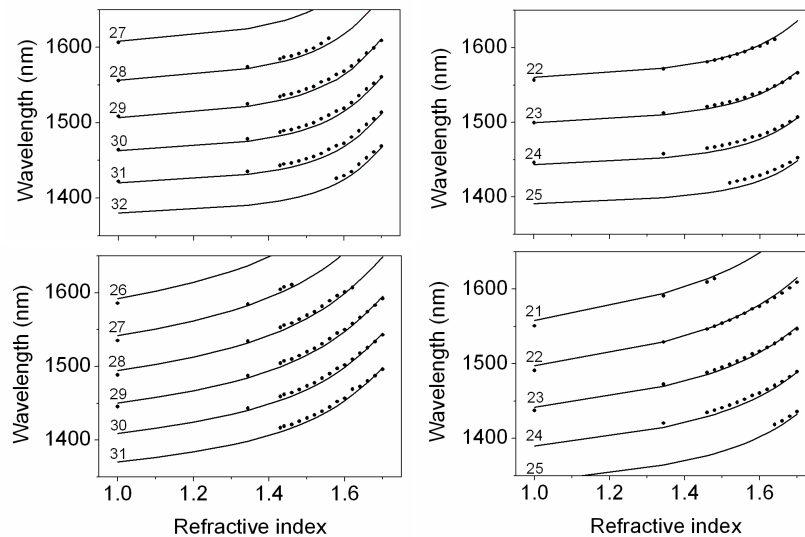


Fig. 4. Calibration of WGM resonances as a function of the refractive index for two thin capillaries: (left) $a = 5.5 \mu\text{m}$ and $d = 0.8 \mu\text{m}$ and (right) $a = 4.5 \mu\text{m}$ and $d = 0.8 \mu\text{m}$. TM^z (top) and TE^z (bottom) WGM resonances. Each resonance is identified with its azimuthal order m .

5. Discussion

The fabrication of small radius capillaries permits to obtain resonators with a free spectral range (FSR) higher than 50 nm. From Fig. 4 we can see that an external radius $a = 5.5 \mu\text{m}$ gives a FSR of 48 nm and $a = 4.5 \mu\text{m}$ gives a FSR higher than 57 nm. Thus, when designing a capillary for a specific applications, it will be possible to adjust the geometrical parameter to have a wide wavelength range with only one resonance. For example, the TM^z resonance with azimuthal order $m = 22$ would be suitable for measuring refractive index changes of a water solution ($n \approx 1.33$) using a wavelength window centered at 1520 nm.

While the FSR is determined basically by the external radius, the response as a function of the refractive index is a function of both the radius and the wall thickness. The solid lines on Fig. 4 are the theoretical response computed after adjusting the wall thickness and a fine adjustment of the external radius. Thus, the adjusted values for a and d are 5.63 and 0.75 μm , for one case, and 4.50 and 0.73 μm for the capillary with smaller external radius. Perhaps, a better concordance could be obtained if it were possible to include the dispersion of the fluids in the simulations, but these data are not available at present. However, a good enough agreement is obtained between experiments and theory.

The importance of using submicron wall thickness capillaries is demonstrated. The experimental slopes around the water refractive index are between 50 and 70 nm/RIU for the

TM^z resonances of the capillaries of Fig. 4, and between 130 and 170 nm/RIU for the TE^z resonances. Thus the sensitivity of WGM resonances of thin capillaries are superior to most previously reported values for other microresonators. However, the low Q factor of the devices that we report here ($Q \approx 500$) makes the detection limit to be worse (between 10^{-3} and 10^{-4} RIU, assuming a wavelength resolution of 1/20th of the linewidth). The preparation of thin capillaries with higher external radius will lead to an improved detection limit, since Q factors as high as 6×10^5 have been reported for capillaries with an external radius of about 100 μm [15]. Although we have not observed any relevant thermal effect, when the Q factor increases thermal stability might be an important issue [21].

In addition, we have demonstrated the feasibility of using these resonators with high refractive index liquids, in particular higher than the refractive index of silica. The spectra of Fig. 3 correspond to an index of 1.52 and in Fig. 4 we can see the response of two capillaries for refractive index values as high as 1.7. The response of these capillaries increases with the refractive index and around 1.6 the slope is higher than 390 nm/RIU, for example for the TE^z resonance of azimuthal order $m = 28$ and radius $a = 5.5 \mu\text{m}$. One could think that, although the resonator can work with a high refractive index, the Q factor might decrease as it happens when the microcavities are immersed in the liquid, but this is not the case. In fact, the Q factor increases with the refractive index of the liquid that fills the inside of the capillaries as one can easily observe in the experimental transmission spectra. In Fig. 5 we can see the spectra for both TM^z and TE^z resonances in air and when the refractive index is 1.7, for the same capillary than in Fig. 4 (right). The Q factors increase from 220 and 120 in air, for the TM^z and the TE^z modes, respectively, up to 520 and 940 when $n = 1.7$. In this figure, when $n = 1.7$, we can observe the second radial order resonances, $l = 2$, which can not be observed at lower refractive index values because the Q is too low. When the liquid has a refractive index higher than that of the wall, it is possible to have total internal reflection in the inner surface of the capillaries and, in the case of thin capillaries, the theory shows a coupling between the modes guided by the external surface and the modes guided by the inner surface. However, the analysis of such a coupling is out of the scope of the present work.

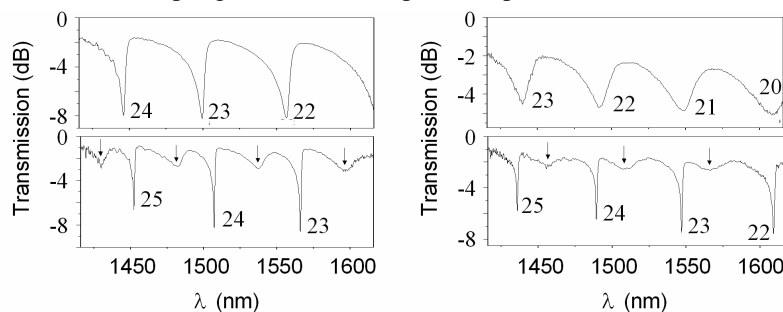


Fig. 5. Transmission spectra for the TM^z (left) and TE^z (right) WGM resonances of a capillary with $a = 4.5 \mu\text{m}$ and $d = 0.8 \mu\text{m}$, when it is filled with air (top) and with a liquid of high refractive index (bottom), $n = 1.7$. Each resonance is identified with its azimuthal order m . The arrows point the second radial order resonances, $l = 2$.

6. Conclusion

We demonstrate that the fabrication of thin capillaries, with submicron wall thickness, is feasible and that they exhibit outstanding characteristics suitable for refractometric sensor applications. The response of these microresonators are higher than 100 nm/RIU for water solutions and can reach values as high as 390 nm/RIU. These microresonators can be used with high refractive index liquids and are readily compatible with microfluidic systems.

Acknowledgments

This work has been financially supported by the Ministerio de Educación y Ciencia (MEC) of Spain (project No. TEC2005-07336-C02-01). V. Zamora acknowledges, as well, financial assistance from FPU grant No. AP-2004-6688.